

# Cycloreversion of Rhenium(V) Diolates Containing the Hydridotris(3,5-dimethylpyrazolyl)borate Ancillary Ligand

Kevin P. Gable,\* Abdullah AbuBaker, Ken Zientara, and Adrian M. Wainwright

Department of Chemistry, Oregon State University, Corvallis, Oregon 97331-4003

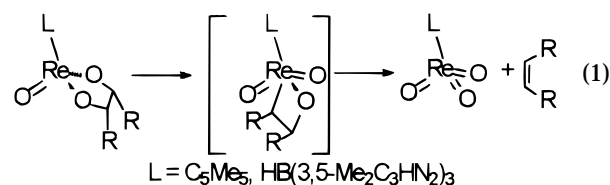
Received September 25, 1998

Hydridotris(3,5-dimethylpyrazolyl)boratorhenium(V) diolates cyclorevert to  $\text{Tp}^*\text{ReO}_3$  and alkene at elevated temperatures in nonpolar solvents. Comparison of activation parameters to those of the analogous pentamethylcyclopentadienyl complexes show the former have similar  $\Delta S^\ddagger$ 's, but higher  $\Delta H^\ddagger$ 's by 2–4 kcal/mol. Computation of the frontier orbitals for this ligand system show that the appropriate acceptor orbital on the metal is pushed to higher energy compared to the case where the ligand is pentamethylcyclopentadienyl, consistent with predictions for the proposed stepwise mechanism of this reaction.

Control of reaction energetics, and particularly reaction rates, is a goal that has long driven chemists. For reactions at metal centers in particular, the ability to modify the electronic structure of the metal center through modification of ancillary ligands has provided an important tool for fine-tuning molecular reactivity.<sup>1</sup> Historically, electronic modification of cyclopentadienyl ligands has been fairly limited: alkylation has been used to introduce both electronic and steric modification of the metal center in a variety of systems.<sup>2,3</sup> More recently, though, pyrazolylborate-based ligands (the quintessential example being the hydridotris(pyrazolyl)borate or Tp ligand) have received attention as possible "Cp equivalents" in that they can be anionic, formal six-electron donors, albeit with substantially different electronic properties.<sup>4</sup> The bonding to the metal in these systems gives much more  $\sigma$  than  $\pi$  character to the ligand–metal interaction than does a cyclopentadienyl ligand. Also, the electronegativity of the nitrogen atom makes these ligands "harder" and presumably renders the metal center less polarizable.<sup>5</sup>

Our interest in the mechanism of rhenium(V) diolate cycloreversion (eq 1) led us to consider the possible effect of ligand modification. We were particularly interested in the degree to which modification of the ancillary  $\text{Cp}^*$  ligand could be used to alter the reaction energetics. This issue is particularly important to the design of new reagents that could be used for synthesis of new C–O bonds. We noted with interest the report that a rhenium

diolate possessing the Klaué ligand ( $\text{CpCo}\{\text{P}(\text{O})(\text{OEt})_2\}_3$ ) extruded alkene with activation parameters almost identical to the corresponding  $\text{Cp}^*$  complex.<sup>6</sup> Cycloreversion of  $\text{TpRe}(\text{O})(\text{diolate})$  complexes had been reported,<sup>7</sup> but no systematic study of reaction energetics had been done. We chose the methylated hydridotris(3,5-dimethylpyrazolyl)borate ligand for this study primarily for the improved solubility of the Re(V) complexes in aromatic organic solvents, but it has the additional feature of probing whether the increased steric congestion resulted in conformational changes and consequent changes in reactivity versus the  $\text{Cp}^*$  compounds we had studied earlier.<sup>8</sup>



Our earlier work favored a stepwise mechanism for cycloreversion involving a rate-determining migration of carbon from oxygen to rhenium, followed by rapid fragmentation of the metallaoxetane. This conclusion was based on several different experimental findings: (a) invariance in the activation enthalpy for extrusion of a series of strained alkenes, arguing against rehybridization of carbon to  $\text{sp}^2$  at the transition state; (b) observation of a significant deuterium kinetic isotope effect, confirming C–O bond reorganization at the transition state; (c) enhanced rates of extrusion for diolates with a large O–O dihedral angle, and diminished rates for those with small O–O dihedrals; (d)

(1) Collman, J. P.; Hegedus, L. S.; Norton, J. S.; Finke, R. F. *Principles and Applications of Organotransition Metal Chemistry*, 2nd ed.; University Science Books: Mill Valley, 1987; Chapter 2.

(2) (a) Gassman, P. G.; Winter, C. H. *J. Am. Chem. Soc.* **1988**, *110*, 6130–6135. (b) Gassman, P. G.; Campbell, W. H.; Macomber, D. W. *Organometallics* **1984**, *3*, 385–387. (c) Gassman, P. G.; Macomber, D. W.; Hershberger, J. W. *Organometallics* **1983**, *2*, 1470–1472.

(3) (a) Richardson, D. E. *Electron-Transfer Reactions: Inorganic, Organometallic and Biological Applications*, Isied, S. S., Ed.; ACS Advances in Chemistry Series 253; American Chemical Society: Washington, DC, 1997; pp 79–90. (b) Richardson, D. E.; Ryan, M. F.; Khan, N. I.; Maxwell, K. A. *J. Am. Chem. Soc.* **1992**, *114*, 10482–10485.

(4) (a) Trofimenko, S. *Chem. Rev.* **1993**, *93*, 943–980. (b) Kitajima, N.; Tolman, W. B. *Progr. Inorg. Chem.* **1995**, *43*, 419–531.

(5) Pearson, R. G. *Hard and Soft Acids and Bases*; Dowden, Hutchinson and Ross: Stroudsburg, PA, 1973.

(6) Cook, J. A.; Davis, W. M.; Davison, A.; Jones, A. G. *Abstracts of the 207th National Meeting of the American Chemical Society*, INOR 0066; American Chemical Society: Washington, DC, 1994.

(7) Thomas, J. A.; Davison, A. *Inorg. Chim. Acta* **1991**, *190*, 231–235.

(8) (a) Gable, K. P.; Phan, T. N. *J. Am. Chem. Soc.* **1994**, *116*, 833–839. (b) Gable, K. P.; Juliette, J. J. *J. Am. Chem. Soc.* **1995**, *117*, 955–962. (c) Gable, K. P.; Juliette, J. J. *J. Am. Chem. Soc.* **1996**, *118*, 2625–2633.

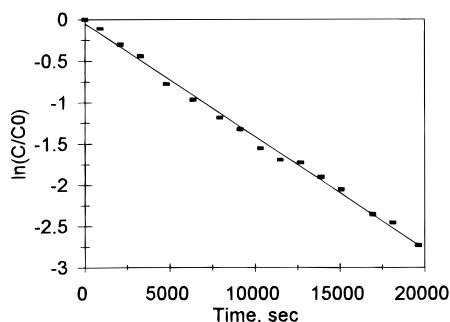
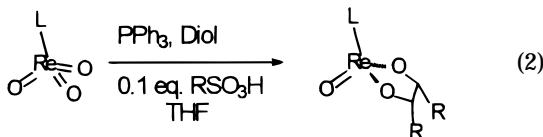


**Figure 1.** First-order kinetic plot for cycloreversion of phenylethanediolate **4**, 104.8 °C. Slope =  $-0.00136$ ; intercept =  $-0.0481$ ,  $r^2 = 0.9955$ .

nonadditivity of substituent effects at the two carbons of the diolate, indicating different degrees of bond reorganization at the two carbons in the transition state. In this work we report that despite a minor difference in reactivity between the two ligand systems, the diolate cycloreversion process is remarkably similar. This is consistent with an orbital-control model we have suggested that is based on a stepwise mechanism.

## Results and Discussion

**Preparation of the Diolate Complexes.** Preparation of the rhenium(V) diolates **1–5** is accomplished using procedures similar to our earlier synthesis of  $\text{Cp}^*\text{Re}$  diolates (eq 2), but is complicated somewhat by the poor solubility of  $\text{Tp}'\text{ReO}_3$  in THF. However, oxygen atom transfer from rhenium to  $\text{PPh}_3$  is complete after 15 h at 50 °C. Santos et al. have reported a similar reduction of a tetrapyrazolylborate complex;<sup>9</sup> although these workers have isolated and partially characterized the Re(V) product, we chose to proceed directly to preparation of the diolate. Cyclocondensation of a vicinal diol with this Re(V) species is best performed simultaneously, or the diol may be added after reduction. Evidence that the trioxo complex is at least sparingly soluble in THF is seen in the successful execution of this procedure with polymer-supported  $\text{PPh}_3$ . After chromatographic workup, the blue diolates were isolated in 20–60% yield (unoptimized in order to maximize purity for subsequent kinetic studies). They could be recrystallized from ethanol/water and were not appreciably air- or water-sensitive.



**Structure of the Diolates.** The structural work that has been done for this class of dialkoxides suggests that rhenium adopts a near-octahedral geometry.<sup>9</sup> The  $^1\text{H}$  NMR spectra of our compounds indicate an average  $C_s$  structure: in *cis*-butane-2,3-diolate **2**, the  $\text{Tp}'$  ligand exhibits four methyl singlets (area ratio 2:2:1:1) and two broadened vinylic singlets (area ratio 2:1);  $C_s$  symmetry is also seen for the diolate portion of the spectrum. Molecular modeling (see Figure 4) suggests that the

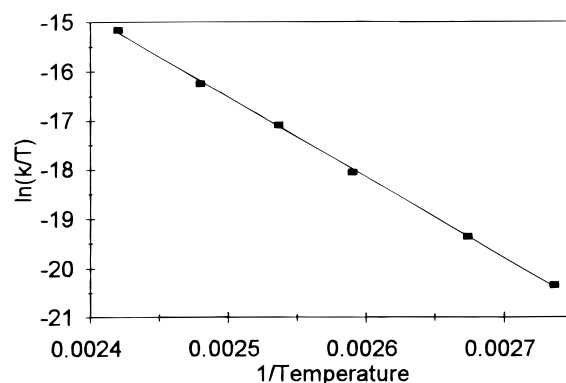


**Figure 2.** Eyring plot for extrusion of ethene from diolate **1**. Slope =  $-16303$ , intercept =  $24.24$ ,  $r^2 = 0.9992$ .

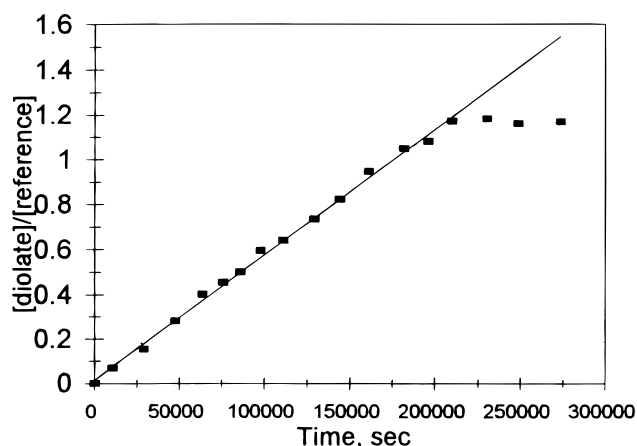


**Figure 3.** Zero-order plot for oxidation of norbornene by  $\text{Tp}'\text{ReO}_3$  at 117 °C. Initial conditions: 5 mg of  $\text{Tp}'\text{ReO}_3$  suspended in 0.5 mL of toluene- $d_8$ ,  $[\text{norbornene}]_0 = 0.14 \text{ M}$ , 1,4-di-*tert*-butylbenzene as integration reference.

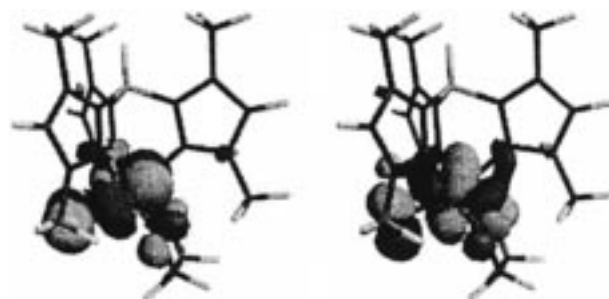


**Figure 4.** Lowest-lying unoccupied orbitals of  $\text{Tp}'\text{Tc}(\text{O}(\text{OCH}_2\text{CH}_2\text{O}))_2$  at the RHF/3-21G\* level. Left, LUMO; right, LUMO+1.

proximal pyrazolyl methyl group forces the diolate to adopt an envelope conformation. However, these observations do not preclude rapid equilibration of  $C_1$  conformers, as is seen for the corresponding  $\text{Cp}^*$  complexes.<sup>8b</sup>

Examination of the coupling between carbinolic C–H protons was undertaken to establish the average solution conformation of the compounds (eq 3). This was accomplished either by explicit deconvolution of the CH multiplet or by iterative simulation and spectral matching. We conclude from the data (Table 1) that interaction of the proximal methyl group does influence the conformation of the ring. For example, we find the *cis* vicinal coupling constants in the ethanediolate **1** are not equal; one is 8.4 Hz, corresponding to a dihedral angle of 17°, while the second is 7.1 Hz, corresponding to a

(9) Paulo, A.; Domingos, A.; Marçalo, J.; Pires de Matos, A.; Santos, I. *Inorg Chem.* **1995**, *34*, 2113–2120.

**Table 1. Vicinal Coupling Constants and Calculated Average H–C–C–H Dihedral Angles**

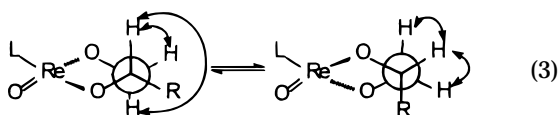
compound	<i>J</i> , Hz	dihedral	dihedral for Cp* diolate
ethanediolate <b>1</b>	8.4	17	34
	7.1	27	34
	6.0	127	120
<i>cis</i> -butanediolate <b>2</b>	6.8	24	38
<i>Z</i> -cyclooctanediolate <b>3</b>	6.0	34	39
phenylethanediolate <b>4</b>	6.7	32	26 (anti)

**Table 2. Activation Enthalpy and Entropy for Alkene Extrusions<sup>a</sup>**

compound	alkene product	$\Delta H^\ddagger$ , kcal/mol	$\Delta S^\ddagger$ , cal/(mol K)	<i>k</i> (373 K), <sup>b</sup> 10 <sup>-5</sup> s <sup>-1</sup>
<b>1</b>	ethene	32.4 ± 0.5	+1.08 ± 1.28	0.14
<b>2</b>	<i>Z</i> -2-butene	33.4 ± 0.6	+3.68 ± 1.61	0.13
<b>3</b>	<i>Z</i> -cyclooctene	29.6 ± 0.3	+0.42 ± 1.69	4.32
<b>4</b>	styrene	27.6 ± 1.6	-3.58 ± 4.55	8.61
<b>5</b>	<i>Z</i> -stilbene	28.9 ± 0.5	0.38 ± 1.43	10.9

<sup>a</sup> Uncertainties are calculated at 95% confidence limits. <sup>b</sup> Calculated on the basis of activation parameters.

27° dihedral angle. (As in our previous work, we utilize the Pachler corrections to the Karplus relationship to account for the electronegativity of substituents.)<sup>10</sup> The larger of these is still smaller than the 34° seen for the Cp\* diolate. Other diolates show small compression of the H–C–C–H dihedral (and, therefore, the O–C–C–O dihedral); these are shown in Table 1. The smaller dihedral angles may arise from compression of the geminal H–C–H angle induced by steric interaction with the pyrazolyl methyl group.



**Kinetics.** Solutions of these diolates in toluene-*d*<sub>8</sub> show first-order reaction to form alkene at temperatures between 90 and 135 °C. The rhenium product Tp'ReO<sub>3</sub> precipitates as a white solid, although small signals in the methyl region of the <sup>1</sup>H NMR (3.00, 2.08 ppm) show it has some slight solubility. Reactant concentrations were measured by including a near-stoichiometric amount of 1,4-di-*tert*-butylbenzene as an integration standard. <sup>1</sup>H NMR spectra of samples were collected using a 30 s relaxation delay to ensure accurate integration. All reactions were followed to at least 3 half-lives; one run for each compound was followed to >4 half-lives to ensure clean first-order behavior. A sample kinetic plot is shown in Figure 1; an example of a typical Eyring plot is shown in Figure 2. Activation parameters and representative rates are in Table 2; full data are included in the Supporting Information.

Several qualitative comparisons between reactions of these Tp'Re diolates and the Cp\* system are identical: simple alkyl substitution has a negligible effect on rate; substitution of a single phenyl group leads to significant acceleration, but a second phenyl group fails to enhance that acceleration. One may conclude, then, that the steric and electronic changes imparted by the Tp' ligand do not significantly alter the mechanistic behavior of the diolate during cycloreversion.

(10) (a) Pachler, K. G. R. *J. Chem. Soc., Perkin Trans. 2* **1972**, 1936–1940. (b) Hasnoot, C. A. G.; de Leeuw, F. A. A.; Altona, C. *Tetrahedron* **1980**, *36*, 2783–2792.

The cycloreversion process for the Tp' complexes must be close to thermoneutral, based on the observation of oxidation of a strained alkene by Tp'ReO<sub>3</sub>, as is likewise seen in the case of the Cp\* compounds.<sup>11</sup> Norbornene reacted with Tp'ReO<sub>3</sub> under similar conditions (toluene-*d*<sub>8</sub>, *T* > 90 °C) to form a diolate. This system showed zero-order kinetics (Figure 3), as expected from the small (constant) solubility of the trioxo complex. Observed zero-order rates could be measured (*k*<sub>obs</sub> = 1.1 × 10<sup>-7</sup> M s<sup>-1</sup> at 390 K; 1.2 × 10<sup>-6</sup> M s<sup>-1</sup> at 413 K). However, because we could not establish to high precision the concentration of trioxo complex under the reaction conditions, we cannot extract a meaningful *k*<sub>ox</sub> from *k*<sub>obs</sub>.<sup>12</sup> Precise estimates of the overall thermodynamics of the system are impossible, for the same reason. However, if we assume a maximum concentration of trioxo of 4 × 10<sup>-3</sup> M, *K*<sub>eq</sub> would be approximately 10, similar to that for oxidation of norbornene by Cp\*ReO<sub>3</sub> (10.5 at 395 K).<sup>11</sup> One expects on the basis of reduction potentials<sup>13</sup> that the thermodynamics are similar to the Cp\* system, perhaps favoring diolate a bit more in the case where the ligand is Tp'; this is consistent with what we can observe.

**Computational Results.** We had earlier suggested that the kinetic barrier for this reaction was controlled by a low-lying acceptor orbital centered on the metal. We therefore wished to make a comparison of the calculated frontier orbitals (especially the LUMOs) for the two systems, to see whether the predicted parallel between activation parameters and orbital energy/topology existed. We chose to use Tc in place of Re<sup>14</sup> to simplify the calculation, as we had in our previous work (see comments below). The geometry was optimized using localized DFT methods in the commercial Spartan computational package,<sup>15</sup> and a final single-point calculation was done at the HF/3-21G\* level for comparison with earlier results for the Cp\* compound. To address whether the results discussed below are entirely an artifact of this relatively crude computational approach, additional work was done at the B3LYP/LANL2DZ level using Gaussian94.<sup>16</sup> The structure of the Cp\* diolate was taken from the published crystal structure;<sup>17</sup> a single-point calculation was performed with this struc-

(11) Gable, K. P.; Phan, T. N. *J. Am. Chem. Soc.* **1993**, *115*, 3036–3037.

(12) Based on the norbornene concentration (0.14 M), we can determine *k*<sub>ox</sub>[Tp'ReO<sub>3</sub>] = 8.0 × 10<sup>-7</sup> M s<sup>-1</sup> (390 K) and 9.2 × 10<sup>-6</sup> M s<sup>-1</sup> (413 K). The Tp'ReO<sub>3</sub> concentration at room temperature can be estimated as approximately (4–6) × 10<sup>-4</sup> M from small peaks visible in the spectra, but the solubility at the elevated temperature of the reaction conditions is unknown, and this renders extraction of *k*<sub>ox</sub> impossible.

(13) Herrmann, W. A.; Kiprof, P.; Rypdal, K.; Tremmel, J.; Blom, R.; Alberto, R.; Behm, J.; Albach, R. W.; Bock, H.; Solouki, B.; Mink, J.; Lichtenberger, D.; Gruhn, N. E. *J. Am. Chem. Soc.* **1991**, *113*, 6527–6537.

(14) Kostlmeier, S.; Nasluzov, V. A.; Herrmann, W. A.; Röscher, N. *Organometallics* **1997**, *16*, 1786–1792.

(15) *Spartan*, v. 4.1.2; Wavefunction, Inc.: 18401 Von Karman Ave., Irvine, CA 92715.

(16) Frisch, M. J.; Trucks, G. W.; Schlegel, H. B.; Gill, P. M. W.; Johnson, B. G.; Robb, M. A.; Cheeseman, J. R.; Keith, T.; Petersson, G. A.; Montgomery, J. A.; Raghavachari, K.; Al-Laham, M. A.; Zakrzewski, V. G.; Ortiz, J. V.; Foresman, J. B.; Cioslowski, J.; Stefanov, B. B.; Nanayakkara, A.; Challacombe, M.; Peng, C. Y.; Ayala, P. Y.; Chen, W.; Wong, M. W.; Andres, J. L.; Replogle, E. S.; Gomperts, R.; Martin, R. L.; Fox, D. J.; Binkley, J. S.; Defrees, D. J.; Baker, J.; Stewart, J. P.; Head-Gordon, M.; Gonzalez, C.; Pople, J. A. *Gaussian 94*, Revision E.1; Gaussian, Inc.: Pittsburgh, PA, 1995.

(17) Herrmann, W. A.; Marz, D. W.; Herdtweck, E. J. *Organomet. Chem.* **1990**, *394*, 285–303.



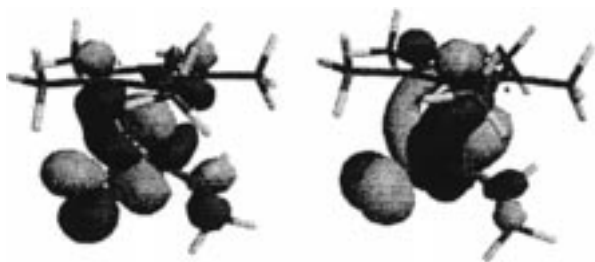


**Figure 5.** Lowest-lying orbital of  $\text{Cp}^*\text{Re}(\text{O})(\text{OCH}_2\text{CH}_2\text{O})$ , at the B3LYP/LANL2DZ level. Left, LUMO; right, LUMO+1.

ture. Since the  $\text{Tp}'$  ligand was too large to model directly, a slightly different model compound was constructed. The metal coordination core geometry was taken from the geometry calculated for the Tc compound. The  $\text{Tp}'$  ligand was replaced with three ammonia ligands; the model complex thus had a net +1 charge (the tetracoordinate borane being absent). The two methods agree entirely with regard to both the relative levels and the nature of the LUMOs, examples of which are displayed in Figures 4 and 5.

Of some concern was that we had to discern a likely geometry of the  $\text{Tp}'$  diolate complex, since no X-ray crystal structures of this compound class have been reported to date. (Our efforts to prepare diffraction-quality crystals have not been successful.) Santos and co-workers have published structures for some related compounds with the tetrakis(pyrazolyl)borate ligand.<sup>9</sup> We found that localized DFT methods gave M=O, M–O, and M–N bond distances for  $\text{Tp}'\text{Tc}(\text{O})(\text{OCH}_2\text{CH}_2\text{O})$  that were comparable to those found for Santos' rhenium bisphenoxide.<sup>18</sup> It is also notable that the DFT optimization identifies a measurable trans influence of the oxo ligand on one M–N bond length (2.238 vs 2.056 and 2.045 Å); this effect has been observed in crystallographic characterizations of related systems.<sup>19</sup>

One possible discrepancy with experimental observation is that the dihedral angles between the hydrogens are predicted to be 10°, less than the 17° and 27° angles projected from the observed coupling constants. The predicted vicinal coupling constants based on the optimized structure (and taking into account averaging due to the ring-flip) are 9.1 and 4.8 Hz; the latter is distinctly smaller than either observed coupling. However, the computed structure illustrates that the orientation of the pyrazole rings is somewhat flexible, in that lateral displacement of the ring trans to the terminal oxo can accommodate the slight puckering of the diolate without inducing a steric clash with the pyrazolyl methyl group. The proximity of these hydrogens was demonstrated through NOE experiments; a 9% enhancement was observed for the carbinolic signal in **2** on irradiation of the upfield methyl singlet in the unique pyrazole. There is also a small enhancement of the H-4 signal in this ring on irradiation of either methyl group. The close-contact distances predicted from the calculated structure are 2.68 and 2.72 Å from methyl to pyrazole H-4; the close contacts from the diolate to the 3-methyl hydrogens are 2.21 and 1.93 Å. No other signal is enhanced on irradiation of either methyl group.

(18) See Supporting Information for comparison of metrical data.

(19) (a) Sundermeyer, J.; Putterlik, J.; Foth, M.; Field, J. S.; Ramesar, N. *Chem. Ber.* **1994**, *127*, 1201–1212. (b) Ref 11.

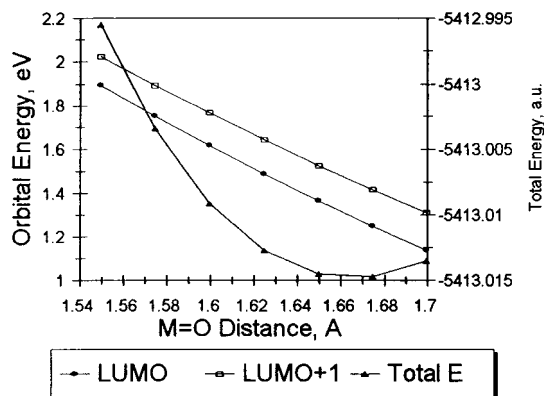


**Figure 6.** Energies of the two LUMOs and total energy as a function of M=O distance for  $\text{Tp}'\text{Tc}(\text{O})(\text{OCH}_2\text{CH}_2\text{O})$ .

The computational results show a striking congruence between the LUMO topologies for  $\text{Cp}^*$  and  $\text{Tp}'$  complexes (Figure 4, Figure 5). There are two low-lying unoccupied orbitals which are primarily M=O  $\pi^*$  antibonding in character, reflecting the triple-bond character of the metal–oxo bond.<sup>20</sup> The order of the two LUMOs of the  $\text{Tp}'$  complex is reversed from that of the  $\text{Cp}^*$  complex: the lower of the two is oriented parallel to the O–O–O plane, while the higher of the two is perpendicular to this plane (Figure 4). There is a general decrease in the energies of all frontier orbitals in the  $\text{Tp}'$  complex; this is perhaps due to the greater electronegativity of the nitrogen atoms in the ligand. (This decrease is consistent with the general stability of these  $d^2$  compounds to air oxidation.)

Since the metal–oxygen antibonding orbitals are strongly dependent on the metal–oxygen bond length (and the strength of the M=O  $\pi$  bond), we systematically varied this parameter to see whether the order of the two orbitals ever changed. Between 1.55 and 1.72 Å, the order of the two orbitals remained constant (all other atom locations held fixed), although their absolute energies varied by as much as 0.8 eV (see Figure 6). Using the geometry of **8** as the basis for the metal coordination geometry raised the total energy by ca. 0.75 eV and lowered each of the LUMOs by ca. 0.1 eV without changing the relative order of the orbitals.

**Mechanistic Implications.** We have previously proposed<sup>8</sup> that these rhenium diolate cycloreversions proceed via rate-determining migration of carbon from oxygen to rhenium, followed by rapid fragmentation of the intermediate metallaoxetane. Although there is no definitive positive evidence requiring the metallaoxetane, this structure is the single species that best fits all the data. Recent theoretical investigations<sup>21</sup> have suggested that for ethylene there are substantially higher barriers to this stepwise reaction processes than for the concerted mechanism, but none of this work

(20) Nugent, W. A.; Mayer, J. M. *Metal–Ligand Multiple Bonds*; Wiley: New York, 1988; pp 21–51.

(21) (a) Pidun, U.; Boehme, C.; Frenking, G. *Angew. Chem., Int. Ed. Engl.* **1996**, *35*, 2817–2820. (b) Dapprich, S.; Ujaque, G.; Maseras, F.; Lledos, A.; Musaev, D. G.; Morokuma, K. *J. Am. Chem. Soc.* **1996**, *118*, 11660–11661. (c) Torrent, M.; Deng, L.; Duran, M.; Sola, M.; Ziegler, T. *Organometallics* **1997**, *16*, 13–19. (d) Pietsch, M. A.; Russo, T. V.; Murphy, R. B.; Martin, R. L.; Rappé, A. K. *Organometallics* **1998**, *17*, 2716–2719.

(22) Nelson, D. W.; Gypser, A.; Ho, P. T.; Kolb, H. C.; Kondo, T.; Kwong, H.-L.; McGrath, D. V.; Rubin, A. E.; Norrby, P.-O.; Gable, K. P.; Sharpless, K. B. *J. Am. Chem. Soc.* **1997**, *119*, 1840–1858.

adequately rationalizes our experimental findings in terms of the behavior of the concerted transition state. Definitive experimental evidence for or against the metallaoxetane will require one such structure be synthesized and the rate of migration and/or alkene loss be compared to the fragmentation rates for diolates. Our discussion here will presume the stepwise process based on our earlier work, although we will consider implications for the concerted mechanism, and for two alternatives.

From the stepwise mechanism and our initial calculations on the pentamethylcyclopentadienylmetal diolates, we suggested that the key step, carbon migration to the metal, might be an orbital-controlled reaction. It follows that the orientation and energy of an appropriate acceptor orbital could be critical for establishing the height of the kinetic barrier for this migration. The experimental and computational results reported here are entirely consistent with this understanding of reactivity. They further agree that in this system the anionic ancillary ligand offers little control of reactivity. The difference that does exist may be due to the slight shift to a stronger  $\sigma$  interaction. The facial arrangement of bonds to the tris(pyrazolyl)borate significantly raises the energy of a pseudo- $t_{2g}$  set of orbitals on the metal. These orbitals are therefore less involved in  $\pi$  bonding to other ligands, and thus the axially oriented acceptor orbital that is a characteristic feature of CpReL<sub>3</sub> compounds is raised in energy. The  $\pi$  bonding to the remaining d orbitals becomes more important, and in this case the orbitals switch in order. (This effect is also a likely contributor to the observed preference for hexacoordinate over heptacoordinate geometries for TpM species, even when the higher-coordinate CpM structures are known to be stable.)<sup>23a</sup>

There are some concerns with the indirect evidence we present here for the physical and electronic structure of the diolate. First, can the diolate achieve a conformation with one or both C–O bonds aligned for migration? The computational optimization suggests the Tp' ligand enforces such an arrangement. There is still some staggering about the C–C bond, confirmed by the NMR results. It is worth noting that the trans effect of the terminal oxo increases the bond length to the pyrazole ring that has the greatest interaction with the diolate, and so the most severe steric interaction is relieved by an important electronic effect. Further, there appears to be some freedom for the pyrazole ring to be slightly deflected laterally to minimize steric clash with the diolate as the diolate ring undergoes ring flipping. Unfortunately, without crystal structure data we are unable to confirm this prediction.

A second concern is whether the (real) rhenium complex is electronically similar to the (modeled) technetium complex. Given the computational expense of modeling the full rhenium compound, we have not fully answered this. However, the truncated version of the complex with ammonia ligands in place of the pyrazole nitrogens showed that, as expected, the LUMO and LUMO+1 were identical to those for the technetium

complex. Hence qualitative arguments based on comparisons for the technetium compounds can be applied to the rhenium compounds.

A final concern is, if both C–O bonds are actually closely parallel (as the calculated structure suggests), does the concerted process become dominant and might this suggest in turn general concerted behavior? This is more difficult to address, in that we have not exhaustively repeated our earlier work and thus lack the same degree of evidence against a concerted process as in the case of the Cp\* compounds. The ligand effect could in principle raise the energy of the stepwise transition state to the point that a concerted process now accelerated by conformational effects takes over. We would have expected a more dramatic change in the electronic effects (see above), particularly on sequential phenyl substitution. (Of note is that in osmylation of alkenes, a reaction claimed to be a concerted cycloaddition on theoretical grounds,<sup>21</sup> comparison of rates for styrene, stilbene, and triphenylethene show significant increases in rate for each additional phenyl ring.)<sup>22</sup> At best we can note the close parallels in substitution effects on the rates and the marginal changes in the apparent average diolate conformation suggested by the NMR as evidence for very little change in mechanism and reactivity upon ligand replacement.

The change in order of the two LUMOs is consistent with the observed kinetic behavior. Because the proposed transition state involves interaction of the C–O bonding electrons with an axially oriented acceptor orbital, perturbation MO theory predicts that the transition-state energy will be controlled by the energies of these two orbitals and by their spatial orientation. If it is necessary to migrate carbon to an axial position, there is a properly oriented acceptor orbital in the Tp' complexes. However, this orbital is no longer the LUMO, and its energy relative to filled orbitals is higher in these compounds than in the Cp\* system. The MO model predicts a somewhat higher kinetic barrier, and this is in fact observed.

At first glance it seems somewhat surprising that this change in ligand has as little effect as it does. The bonding between Cp\* and a metal is highly delocalized; the Tp' ligand ought to exhibit more directional,  $\sigma$  character in its interaction with the metal. The observation that the behavior of these compounds is so similar to that of the Cp\* compounds strongly indicates that the controlling elements lie elsewhere. It is also worth noting that there is some disagreement in the literature whether this ligand change affects metal electronic structure more strongly than it does the steric environment.<sup>23</sup>

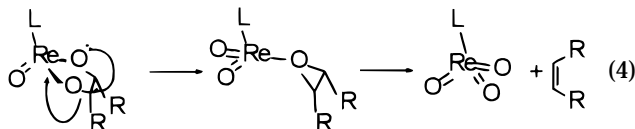
Given the nature of the acceptor orbitals, though, it is easy to see why our initial expectation of a dramatic change in energetics was not realized. Note that both of these are primarily metal–oxo antibonding. There is very little contribution from the ancillary ligand for either the Cp\* or Tp' system. The influence of this ancillary ligand is indirect; the absolute energies of all comparable orbitals are lower for L = Tp' than for Cp\*. This might be ascribed to the hardness of the N–M interaction; localization of the ligand–metal bonds and the electronegativity of the nitrogens probably play a role. Alternatively, it may reflect a stronger L–M

(23) (a) Curtis, M. D.; Shiu, K.-B.; Butler, W. M. *J. Am. Chem. Soc.* **1986**, *108*, 1550–1561. (b) Skagestad, V.; Tilset, M. *J. Am. Chem. Soc.* **1993**, *115*, 5077–5083. (c) Etienne, M.; White, P. S.; Templeton, J. L. *Organometallics* **1993**, *12*, 4010–4015. (d) Janiak, C. *Chem. Ber.* **1994**, *127*, 1379–1385.



bonding interaction. However, the nature of the ligand(s) that are directly involved in the acceptor orbital should play a more important role.

Finally, there are additional mechanistic hypotheses to be considered. One would be migration of carbon to oxygen rather than to rhenium (eq 4). This would result in an epoxide coordinated to a Re(V) center, which then might undergo concerted fragmentation. This mechanism has some support in that methylrhenium dioxide reacts with epoxides to form diolates;<sup>24</sup> we have also considered this a possibility based on the reaction of  $\{\text{Cp}^*\text{ReO}_2\}_2$  with epoxides to form alkenes and  $\text{Cp}^*\text{ReO}_3$ .<sup>25</sup> However, the methyl complex is much more Lewis acidic than either the  $\text{Cp}^*$  or  $\text{Tp}'$  complexes. It is extremely difficult in the case of either the  $\text{Tp}'$  or  $\text{Cp}^*$  diolates to locate appropriate orbital overlap with oxygen lone pairs for such a migration, but the slight conformational change imposed by the  $\text{Tp}'$  ligand could offer a rationale for the increase in  $\Delta H^\ddagger$ . There is no evidence to rigorously exclude this path.



A minor variant of any mechanism for these systems would be to decomplex part of the ancillary ligand, either by ring slipping ( $\eta^5 \rightarrow \eta^3$  or  $\eta^1$ ) of the cyclopentadienyl or by loss of an Re–N bond ( $\kappa^3 \rightarrow \kappa^2$ ) for the  $\text{Tp}'$  ligand. This process by itself cannot be the rate-limiting step, given the observation of a significant secondary deuterium isotope effect for the  $\text{Cp}^*$  diolates. On one hand, there is no direct evidence to preclude such a process accompanying the C–O bond cleavage. However, it seems to require an extraordinary coincidence that as dramatic a change in ligand as we have made in this study should have no more effect than it does if such ligand slippage is an important feature of the mechanism.

## Experimental Section

**General Methods.** All reactions were performed under nitrogen using a double-manifold Schlenk line. THF, diethyl ether, and toluene were distilled from sodium/benzophenone ketyl. Hexane was distilled from Na/K. NMR spectra were obtained on either a Bruker AC 300 (operating at 300.133 MHz for proton or 75.409 MHz for carbon) or a Bruker AM 400 (operating at 400.134 MHz for proton or 100.614 MHz for carbon) spectrometer. All chemical shifts were referenced to residual proton or carbon in solvent and expressed in ppm downfield from tetramethylsilane. Infrared spectra were run on a Nicolet 510P spectrometer.

$\text{Tp}'\text{ReO}_3$  was prepared according to the method of Herrmann et al.<sup>26</sup> *cis*-1,2-Cyclooctanediol, 1,4-di-*tert*-butylbenzene, *meso*-2,3-butanediol, *meso*-hydrobenzoin, methanesulfonic acid, and polymer-supported triphenylphosphine were used as received from Aldrich. Molecular sieves (beads, 4 Å, Fisher) were crushed in a mortar and pestle and dried in a 100 °C oven for

at least 15 h. Elemental analyses were performed by Texas Analytical Laboratories.

**General Procedure for the Diolate Synthesis.**  $\text{Tp}'\text{ReO}_3$  (100 mg, 0.188 mmol), polymer-supported triphenylphosphine (78 mg, 0.24 mmol P), methanesulfonic acid (2.0 mg, 0.021 mmol), ground molecular sieves (1.5 g), and diol (0.430 mmol) were allowed to stir at room temperature for at least 15 h in 25 mL of THF. The solution was filtered, and the solvent was removed in vacuo. The product was purified either by crystallization from ethanol/water or by chromatography on silica gel (Scientific Adsorbents Inc, 32-63). Initial elution with 1:1 dichloromethane/hexane was used to remove unreacted diol. Dichloromethane/hexane (3:1) or chloroform was used to elute the blue diolate.

**Hydridotrakis(3,5-dimethyl-1-pyrazolyl)borato(ethane-1,2-diolato)(oxo)rhenium(V) (1).** Yield from 50 mg of  $\text{Tp}'\text{ReO}_3$ : 20 mg (0.03 mmol, 38%) of sky-blue solid.  $^1\text{H}$  NMR (toluene-*d*<sub>6</sub>):  $\delta$  1.90 (s, 3H), 2.21 (s, 6H), 2.29 (s, 3H), 2.73 (s, 6H), 5.09 (m, 2H), 5.12 (s, 1H), 5.35 (m, 2H), 5.56 (s, 2H).

**Hydridotrakis(3,5-dimethyl-1-pyrazolyl)borato(*cis*-butane-1,2-diolato)(oxo)rhenium(V) (2).** Yield from 100 mg of  $\text{Tp}'\text{ReO}_3$ : 65 mg (0.11 mmol, 59%) of blue solid.  $^1\text{H}$  NMR (toluene-*d*<sub>6</sub>):  $\delta$  1.35 (d, 6H), 1.91 (s, 3H), 2.21 (s, 6H), 2.35 (s, 3H), 2.74 (s, 6H), 5.15 (s, 1H), 5.55 (m, 2H), 5.57 (s, 2H).  $^{13}\text{C}$  NMR (toluene-*d*<sub>6</sub>):  $\delta$  12.1, 12.25, 13.75, 14.1, 18.1, 91.42, 106.84, 107.46, 142.1, 146.37, 153, 157. IR (KBr): 2963, 1545, 1452.6, 1383, 1205.7, 1072.6, 958.74, 908.59, 864, 817.9, 769.7, 692.6, 642.4. Anal. Calcd for  $\text{C}_{19}\text{H}_{30}\text{BN}_6\text{O}_3\text{Re}$ : C, 38.84; H, 5.14; N, 14.30. Found: C, 38.80; H, 5.12; N, 14.16.

**Hydridotrakis(3,5-dimethyl-1-pyrazolyl)borato(*cis*-cyclooctane-1,2-diolato)(oxo)rhenium(V) (3).** Yield from 100 mg of  $\text{Tp}'\text{ReO}_3$ : 60 mg (0.094 mmol, 50%) of blue solid.  $^1\text{H}$  NMR (toluene-*d*<sub>6</sub>):  $\delta$  1.45 (m, 2H), 1.68 (m, 2H), 1.92 (s, 3H), 2.02 (m, 1H), 2.23 (s, 6H), 2.3 (m, 1H), 2.4 (s, 3H), 2.75 (s, 6H), 5.15 (s, 1H), 5.55 (m, 2H), and 5.6 (s, 2H).  $^{13}\text{C}$  NMR (toluene-*d*<sub>6</sub>):  $\delta$  12.1, 12.30, 13.9, 14.4, 23.1, 26.7, 32.3, 97.7, 106.9, 107.4, 142.1, 146.3, 153, 157. IR (KBr): 2928.4, 1545, 1452.6, 1383, 1205.7, 1072.6, 964.5, 943.3, 817.9, 669.38. Anal. Calcd for  $\text{C}_{23}\text{H}_{36}\text{BN}_6\text{O}_3\text{Re}$ : C, 43.05; H, 5.65; N, 13.09. Found: C, 42.87; H, 5.67; N, 13.03.

**Hydridotrakis(3,5-dimethyl-1-pyrazolyl)borato(phenyl-1,2-diolato)(oxo)rhenium(V) (4).** Yield from 100 mg of  $\text{Tp}'\text{ReO}_3$ : 40 mg (0.063 mmol, 33%) of blue solid.  $^1\text{H}$  NMR ( $\text{CDCl}_3$ ):  $\delta$  2.15 (s, 3H), 2.45 (s, 3H), 2.54 (s, 3H), 2.57 (s, 3H), 2.65 (s, 6H), 4.6 (t, 1H), 5.55 (s, 1H), 5.7 (dd, 1H), 5.95 (s, 2H), 6.25 (dd, 1H), 7.4–7.2 (m, 5H).  $^{13}\text{C}$  NMR ( $\text{CDCl}_3$ ):  $\delta$  12.56, 12.69, 12.78, 14.05, 14.55, 14.62, 94.83, 96.31, 107.53, 107.63, 127.5, 127.7, 128.3, 143.0, 146.47, 146.97, 147.73, 153.7, 156.8, 157.5. IR (KBr): 2924.5, 1545, 1452.6, 1205.7, 1072.6, 995.4, 958.7, 922, 864, 819.8, 677. Anal. Calcd for  $\text{C}_{23}\text{H}_{30}\text{BN}_6\text{O}_3\text{Re}$ : C, 43.46; H, 4.75; N, 13.22. Found: C, 43.41; H, 4.73; N, 13.18.

**Hydridotrakis(3,5-dimethyl-1-pyrazolyl)borato(*cis*-1,2-diphenyl-1,2-diolato)(oxo)rhenium(V) (5).** Yield from 100 mg of  $\text{Tp}'\text{ReO}_3$ : 27 mg (0.038 mmol, 20%) of blue solid.  $^1\text{H}$  NMR ( $\text{CDCl}_3$ ):  $\delta$  2.3 (s, 3H), 2.52 (s, 3H), 2.55 (s, 6H), 2.65 (s, 6H), 5.55 (s, 1H), 5.65 (s, 2H), 5.95 (s, 2H), 7.3–6.8 (m, 10H).  $^{13}\text{C}$  NMR ( $\text{CDCl}_3$ ):  $\delta$  12.79, 12.82, 13.94, 14.76, 100.82, 107.47, 108.0, 126.26, 127.2, 128.1, 143.1, 145.55, 147.31, 152.8, 157.23. IR (KBr): 2924.5, 1545, 1452.6, 1207.6, 1070.6, 910.5, 696.4. Anal. Calcd for  $\text{C}_{29}\text{H}_{34}\text{BN}_6\text{O}_3\text{Re}$ : C, 48.94; H, 4.81; N, 11.80. Found: C, 49.03; H, 4.87; N, 11.85.

**Hydridotrakis(3,5-dimethyl-1-pyrazolyl)borato(*cis*-2,3-norbornanediolato)(oxo)rhenium(V) (5).**  $\text{Tp}'\text{ReO}_3$  (10 mg, 0.02 mmol) and norbornene (100 mg, 1.06 mmol) were mixed in 1.0 mL of pyridine and sealed under vacuum. The reaction mixture was heated to 105 °C for 15 h, then chromatographed (silica;  $\text{CHCl}_3$ ). Approximately 10 mg of blue solid was isolated.  $^1\text{H}$  NMR ( $\text{C}_6\text{D}_6$ ): 5.57 (s, 2H), 5.30 (s, 2H), 5.20 (s, 1H), 2.90

(24) Zhu, Z.; Al-Ajlouni, A. M.; Espenson, J. H. *Inorg. Chem.* **1996**, *35*, 1408–1409.

(25) Gable, K. P.; Gartman, M. A.; Juliette, J. J. *Organometallics* **1995**, *14*, 3138–3140.

(26) (a) Degnan, I. A.; Herrmann, W. A.; Herdtweck, E. *Chem. Ber.* **1990**, *123*, 1347–1349. (b) Coe, B. J. *Polyhedron* **1992**, *11*, 1085–1091.

(d, 1H,  $J = 15$  Hz), 2.87 (s, 6H), 2.80 (br. s, 2H), 2.35 (s, 3H), 2.17 (s, 6H), 1.87 (s, 3H), 1.1–1.4 (m, 5H).  $^{13}\text{C}$  NMR ( $\text{C}_6\text{D}_6$ ): 157.2, 152.6, 146.3, 142.5, 107.5, 106.8, 102.9, 46.4, 34.4, 30.2, 26.8, 14.3, 14.2, 12.2.

**Measurement of Kinetics.** For extrusion of alkene from diolates, 0.03 M solutions of diolate were prepared under  $\text{N}_2$  in  $\text{C}_7\text{D}_8$ . An amount of 1,4-di-*tert*-butylbenzene sufficient to make the solution approximately 0.02 M was added. Samples were sealed in NMR tubes under vacuum. These were heated in a thermostated bath; temperature was measured with calibrated thermometers to  $\pm 0.1$  °C. The sample tube was periodically removed and cooled to 25 °C, and the NMR spectrum was recorded to obtain at least four data points every half-life for 4 half-lives. A relaxation delay of 30 s was used in collecting NMR spectra to ensure accurate integration.

Neither intermediates nor byproducts were observed. Measurement of the methyl groups of the ligand in the reactant was referenced to the di-*tert*-butylbenzene peaks as a measure of relative concentration. Plotting  $\ln([\text{diolate}]/[\text{diolate}]_0)$  versus time gave linear plots ( $r^2 > 0.99$ ) with slope =  $-k_{\text{obs}} = -k_e$ .

For oxidation of norbornene, a suspension of  $\text{Tp}^*\text{ReO}_3$  (typically 5 mg/0.5 mL) in  $\text{C}_7\text{D}_8$  was prepared. A known mass of 1,4-di-*tert*-butylbenzene was added so as to give approximately a 0.02 M solution. To this was added norbornene (final concentration 0.14 M); the sample was sealed under vacuum. The initial concentration of alkenes was determined by NMR relative to 1,4-di-*tert*-butylbenzene. Relaxation delays of up to 30 s were used to ensure accurate integration. Tubes were heated in a thermostated bath as above. Periodically, the tube was removed and the NMR spectrum measured. A pseudo-zero-order plot of  $[\text{diolate}]_{\text{rel}}$  versus  $t$  was observed (Figure 3) for most of the reaction prior to establishment of equilibrium, where the  $[\text{diolate}]/[\text{norbornene}]$  ratio was 0.035. Small methyl peaks for  $\text{Tp}^*\text{ReO}_3$  were observed at  $\delta$  2.995 and 2.085; these indicated a room-temperature solubility of  $(4-6) \times 10^{-4}$  M by comparison with the internal standard.

**Computations.** Geometry optimizations for Tc complexes were performed using Spartan v. 4.1.2<sup>15,27</sup> using the DN\* basis set and a fine grid mesh, with energies based on the local spin density functional of Vosko, Wilk, and Nusair.<sup>28</sup> The geometries to which these DFT calculations converged were then used to perform a single-point calculation at the RHF/3-21G\* level. The M=O bond was then systematically varied from the optimum distance, using 8 points over a bond distance range of 1.55–1.72 Å, again performing a single-point calculation for each geometry at the RHF/3-21G\* level.

Computations for rhenium compounds were performed using Gaussian94.<sup>16</sup> Becke's three-parameter hybrid method,<sup>29</sup> using the LYP correlation functional,<sup>30</sup> was used. Single-point calculations were performed using either a published solid-state structure<sup>17</sup> or a modification of the optimized structure for a Tc complex (from above) in which the tris(pyrazoly)borate had been replaced with three ammonia ligands, keeping the M–N bond lengths fixed.

**Acknowledgment.** We wish to thank the National Science Foundation (CHE-9312650, 9619296) and the donors to the Petroleum Research Fund, administered by the American Chemical Society, for support of this work.

**Supporting Information Available:** Table of observed rate constants and comparison of calculated metrical parameters for  $\text{Tp}^*\text{Tc}(\text{O})(\text{OCH}_2\text{CH}_2\text{O})$  with published structural data (3 pages). See any current masthead page for ordering information and Web access instructions.

#### OM980807O

(27) (a) Hohenberg, P.; Kohn, W. *Phys. Rev.* **1964**, *136*, B864–B871. (b) Kohn, W.; Sham, L. S. *Phys. Rev.* **1965**, *140*, A1133–A1138.

(28) Vosko, S. H.; Wilk, L.; Nusair, M. *Can. J. Phys.* **1980**, *58*, 1200–1211.

(29) Becke, A. D. *J. Chem. Phys.* **1993**, *98*, 5648–5652.

(30) Lee, C.; Yang, W.; Parr, R. G. *Phys. Rev. B* **1988**, *37*, 785–789.